

## Microwave Spectroscopy Evidence of Superconducting Pairing in the Magnetic-Field-Induced Metallic State of $\text{InO}_x$ Films at Zero Temperature

Wei Liu,<sup>1</sup> LiDong Pan,<sup>1</sup> Jiajia Wen,<sup>1</sup> Minsoo Kim,<sup>2</sup> G. Sambandamurthy,<sup>2</sup> and N. P. Armitage<sup>1</sup>

<sup>1</sup>*Department of Physics and Astronomy, Johns Hopkins University, 3400 North Charles Street, Baltimore, Maryland 21218, USA*

<sup>2</sup>*Department of Physics, University at Buffalo-SUNY, 239 Fronczak Hall, Buffalo, New York 14260, USA*

(Received 3 September 2012; published 8 August 2013)

We investigate the field-tuned quantum phase transition in a 2D low-disorder amorphous  $\text{InO}_x$  film in the frequency range of 0.05 to 16 GHz employing microwave spectroscopy. In the zero-temperature limit, the ac data are consistent with a scenario where this transition is from a superconductor to a metal instead of a direct transition to an insulator. The intervening metallic phase is unusual with a small but finite resistance that is much smaller than the normal state sheet resistance at the lowest measured temperatures. Moreover, it exhibits a superconducting response on short length and time scales while global superconductivity is destroyed. We present evidence that the true quantum critical point of this 2D superconductor metal transition is located at a field  $B_{\text{sm}}$  far below the conventionally defined critical field  $B_{\text{cross}}$  where different isotherms of magnetoresistance cross each other. The superfluid stiffness in the low-frequency limit and the superconducting fluctuation frequency from opposite sides of the transition both vanish at  $B \approx B_{\text{sm}}$ . The lack of evidence for finite-frequency superfluid stiffness surviving  $B_{\text{cross}}$  signifies that  $B_{\text{cross}}$  is a crossover above which superconducting fluctuations make a vanishing contribution to dc and ac measurements.

DOI: [10.1103/PhysRevLett.111.067003](https://doi.org/10.1103/PhysRevLett.111.067003)

PACS numbers: 74.78.-w, 74.25.Dw, 74.25.Gz, 74.40.Kb

The conventional wisdom is that metallic states are prohibited at  $T = 0$  in two-dimensional (2D) systems with finite disorder due to Anderson localization [1]. The possible ground states for 2D disordered systems with superconducting correlations are superconductors and insulators. The 2D superconductor-insulator transition (SIT) between the two ground states is a paradigmatic example of a continuous quantum phase transition (QPT), where the transition is induced by changing a nonthermal parameter at zero temperature. It has been the subject of many theoretical and experimental studies, especially in the presence of magnetic field [2–6]. One possible scenario is that this transition occurs by destroying the amplitude of the superconducting order parameter [2]. Another possibility is that the Cooper pairs lose global phase coherence across the transition [3]. In this case, one expects Cooper pairs to exist even in the insulator, but they are localized.

Within the bosonic description, a zero-temperature metallic state can only exist at the quantum critical point (QCP) with a universal resistance of order  $R_Q = h/4e^2 \approx 6450 \Omega$ . Although some indications for superconducting pairing in the insulator have been reported [7–11], there has been little definitive evidence in favor of this pure bosonic model. Moreover, a widely observed phenomenon that cannot be explained by either scenario is the apparent existence of 2D zero-temperature metallic ground states in many experiments of disordered thin films [12–19], Josephson junction arrays [20], artificially patterned superconducting islands [21], and interface superconductivity [22,23]. In this metallic state, the sheet resistances ( $R_{\square}$ )

first drop when lowering the temperature. As  $T \rightarrow 0$ ,  $R_{\square}$  becomes temperature independent and saturates at a nonzero value that is much lower than the normal state sheet resistance  $R_N$ , indicating the existence of a separate metallic phase in the phase diagram. This effect is usually most pronounced in low-disorder films that feature a critical sheet resistance (its value at the QCP) much lower than  $R_Q$  [14,24].

Despite many theoretical efforts to demonstrate the possibility of a zero-temperature dissipative state with superconducting correlations [15,25–29], the nature of this intermediate metallic phase is still under debate. A true metallic phase with superconducting correlations may be surprising because one might naively expect that delocalized Cooper pairs or vortices would ultimately condense at zero temperature. On the experimental side, many groups have focused only on dc transport. ac measurements give an advantage in studying the 2D SIT in that one can be explicitly sensitive to temporal correlations. ac spectroscopy may reveal the true location of the QCP since it provides information about the critical slowing down of the characteristic frequency scales approaching a transition. Through the imaginary conductance, microwave measurements of superconductors also allow access to the superfluid stiffness  $T_{\theta}(\omega)$ , which is related to the superconducting response on a length scale set by the probing frequency.

In this Letter, we present novel measurements of frequency, temperature, and field dependence of the complex microwave conductance on a low-disorder 2D superconducting  $\text{InO}_x$  film through its QPT. Above a field

$B_{sm} \approx 3$  Tesla, superconducting fluctuations are observed in a state with small but finite resistance as  $T \rightarrow 0$ . Our main finding is that  $B_{sm}$  is the true QCP for a transition from a 2D superconductor to an anomalous 2D metal at  $T \rightarrow 0$ . This metallic phase is unusual due to the survival of the superconducting correlations on short length scales at fields right above  $B_{sm}$ . From the simultaneously measured dc sheet resistance  $R_{\square}$ , a well-defined field  $B_{cross} \approx 7.5$  Tesla is identified as the crossing point of different isotherms  $R(B)$ . According to scaling theories of the resistance curves,  $B_{cross}$  is conventionally interpreted to be the QCP of a 2D SIT [3,30,31]. Contrary to the expectations for the slowing down of the fluctuations near the presumed critical field  $B_{cross}$ , the relevant frequency scale extrapolates to zero at the much smaller field  $B_{sm}$ . The superfluid stiffness  $T_{\theta}$  in the zero-frequency limit vanishes from the superconducting side also at  $B_{sm}$ , suggesting the loss of global superconductivity near  $B_{sm}$ .  $T_{\theta}$  approaches zero at  $B \approx B_{cross}$  in the high-frequency limit, indicating  $B_{cross}$  only signifies a crossover to a regime where superconducting correlations are strongly suppressed even at short length scales.

Broadband microwave experiments were performed in a home-built Corbino microwave spectrometer coupled into a He-3 cryostat [32,33]. Samples are morphologically homogeneous  $\text{InO}_x$  films, and the nominal 2D QPT can be tuned by applying perpendicular magnetic fields [7,10,24,34]. We measured the complex reflectivity of the sample, from which complex sheet impedance and conductance can be obtained. Three calibration samples with known reflection coefficients [33] were measured to remove the contributions from the coaxial cables to the reflected signals [32,35–39]. Two-terminal dc resistances can be simultaneously measured via a bias tee. The dc resistance without microwave illumination was used to check and correct for any microwave induced heating [33]. Calibrations were performed at each displayed magnetic field unless otherwise specified. With substrate corrections [33], the true response of the  $\text{InO}_x$  film can be isolated at all fields and temperatures.

In Fig. 1(a), we plot the two-terminal sheet resistance  $R_{\square}$  as a function of temperature at fixed magnetic fields. The  $\text{InO}_x$  film studied in this Letter shows a transition to a zero resistance state at  $T_c = 2.36$  K at zero field. Previous microwave studies have demonstrated that its zero-field transitions due to thermal fluctuations are consistent with a 2D Kosterlitz-Thouless-Berezinskii type [39]. At low temperatures, the slopes of the resistance curves change sign at about 7.5 Tesla [see Fig. 1(a)]. For the two lowest temperatures, the data also exhibit an isoresistance crossing point at 7.5 Tesla. Both observations seem to be consistent with previous dc measurements of  $\text{InO}_x$ , suggesting  $B_{cross}$  as the QCP [40]. Comparing our resistance curves with the ones from  $a$ -MoGe [14] and interface superconductivity [22], we find that except for the differences in  $T_c$

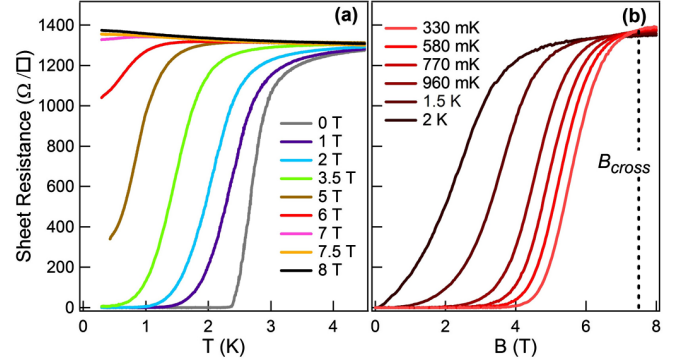


FIG. 1 (color online). (a) Temperature dependence of the sheet resistance  $R_{\square}$  at different fields as indicated by the color legend. (b)  $R_{\square}$  as a function of field at six fixed temperatures as shown by the color legend. The crossing point of the two lowest-temperature isotherms is approximately 7.5 Tesla.

and  $B_{cross}$ , these sets of resistance curves of three very different systems look very similar in that they all exhibit (1) an  $R_N$  that is much smaller than  $R_Q$ , (2) an exceedingly weak “insulating state” with barely a 10% rise in the resistance from 4 K to the lowest measured temperatures at  $B > B_{cross}$ , and (3) an apparent trend toward saturation in  $R_{\square}$  toward zero temperatures for fields below  $B_{cross}$ . This saturation in the  $\text{InO}_x$  film was confirmed in separate two-terminal measurements down to 60 mK [33]. This implies that this  $\text{InO}_x$  is very different from strongly disordered ones that show an enhancement of the resistance upward of  $10^9 \Omega$  with applied magnetic fields at low temperatures [7,10]. We can characterize the effective disorder level using the product of Fermi wave vector ( $k_F$ ) and electronic mean free path ( $l$ ) [33], which is in the range 3–6 for this sample. It implies that this film has a much lower disorder level and falls into the same class of 2D lower-disorder superconducting thin films that usually feature a transition into a metallic phase out of the superconducting state at  $T \rightarrow 0$  [24].

In Figs. 2(a) and 2(b), we plot the real ( $G_1$ ) and imaginary ( $G_2$ ) conductances as a function of frequency at the base temperatures for each field ( $\approx 426$  mK for 5 Tesla and  $\approx 300$  mK for all other fields) [33]. As shown by the straight line with a slope of  $-1$  on the log-log plot in Fig. 2(b), at zero field and 300 mK,  $G_2$  shows the  $1/\omega$  frequency dependence expected for a superconductor at frequencies below the superconducting gap ( $2\Delta \approx 170$  GHz). This dependence is consistent with  $G_1 = (\pi/2)(N_s e^2 d/m)\delta(\omega)$  via the Kramers-Kronig relation, where  $N_s$  is the superfluid density and  $d$  is the sample thickness. Indeed,  $G_1$  at zero field is small with a value that is at the limit of our experimental sensitivity [32,33]. For  $B \ll B_{cross}$ ,  $G_2$  falls as the field is applied but remains linear with the same slope in the log-log plot. This implies that the  $\delta$  function in  $G_1$  is preserved, although its spectral weight (proportional to the superfluid density) is decreasing.

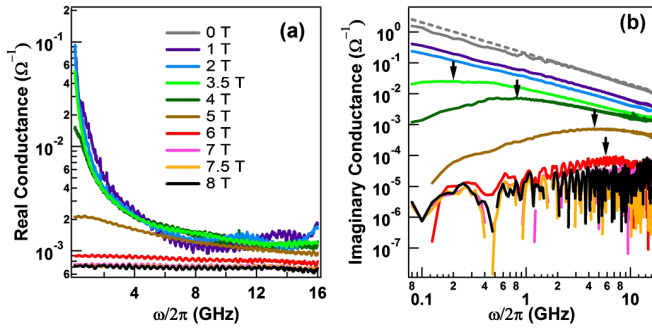


FIG. 2 (color online). Frequency dependence of the (a) real ( $G_1$ ) and (b) imaginary ( $G_2$ ) conductances, respectively, in the ranges  $\omega/2\pi = 0.08$ –16 GHz at the base temperature for each field.  $G_1$  and  $G_2$  have the same color legend at finite fields, except that  $G_1$  at zero field is not plotted. The dashed grey line in (b) is a guide to the eye for  $G_2 \propto 1/\omega$ . Arrows in (b) mark the frequencies of the maxima in  $G_2$ .

At intermediate-field strengths ( $B \approx 3.5$  Tesla), a maximum in  $G_2$  appears [see the arrows in Fig. 2(b)]. According to the Kramers-Kronig relation, this implies that a significant spectral component in  $G_1$  has a finite width. As shown previously [39], the frequency of the maximum in  $G_2$  corresponds to the characteristic fluctuation rate  $\Omega$  in a fluctuating superconductor. The decrease in the frequency of the peak in  $G_2$  as the field is reduced is an unambiguous signature of the critical slowing down of the fluctuation frequency while approaching a continuous transition. However, the peak in  $G_2$  is developed at a field that is well below  $B_{\text{cross}}$  and the fluctuations are clearly *speeding up* as we approach  $B_{\text{cross}}$  from below. This behavior is inconsistent with the conventional wisdom for QPT phenomenologies if  $B_{\text{cross}}$  is a QCP because one generally expects a *slowing down* of the fluctuation frequency scales near a continuous transition. When  $B \approx B_{\text{cross}}$ , we cannot distinguish the superconducting signal from the normal state background as  $G_1$  is flat and featureless and  $G_2$  is small.

An essential quantity for analyzing superconducting fluctuations is the superfluid stiffness  $T_\theta$ , which is the energy scale required to twist the phase of the superconducting order parameter. Within a parabolic band approximation,  $T_\theta \propto N_s$  represents the superfluid density. More precisely (and in a model independent fashion), it is proportional to the spectral weight in the superconducting response and can be measured through  $G_2$  as  $T_\theta(\omega) = (G_2(\omega)/G_Q)(\hbar\omega/k_B)$ , where  $G_Q = 1/R_Q$ . This relation expresses the energy scale  $T_\theta$  in degrees Kelvin and gives the superfluid stiffness on a length scale set by the probing frequency. Figure 3(a) shows  $T_\theta(\omega)$  at the respective base temperatures described above for each field. At zero field,  $T_\theta$  shows essentially no frequency dependence, which suggests that the phase is ordered on all lengths. At  $B \ll B_{\text{cross}}$ ,  $T_\theta$  drops but remains frequency independent. For intermediate fields,  $T_\theta$  starts

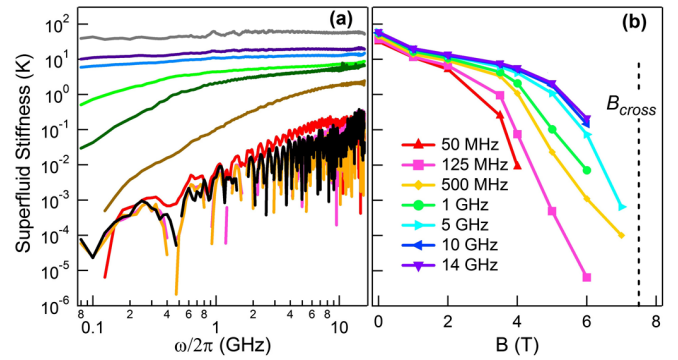


FIG. 3 (color online). (a) Frequency dependence of the superfluid stiffness in the ranges  $\omega/2\pi = 0.08$ –16 GHz at the base temperature for each field. The color legend for fields is the same as in Fig. 2(a). (b) Superfluid stiffness as a function of field at different frequencies at the base temperature for each field.

to acquire a strong frequency dependence at low  $\omega$ , which reflects that Cooper pairs have short-range correlations that can be resolved at high probing frequency while the long-range correlations are suppressed. At high  $\omega$ , the frequency dependence becomes less pronounced, showing that one approaches a well-defined high-frequency limit.

The rapid decrease in the overall scale of  $T_\theta$  can be clearly observed in Fig. 3(b), where we display the field dependence of  $T_\theta$  at several frequency cuts from Fig. 3(a). Above 2 Tesla, the curves start to spread, indicating the superconducting correlations gain a length dependence. At the lowest frequency (50 MHz, which probes the longest length scale),  $T_\theta$  drops around 3 Tesla, indicating that long-range ordered phase coherence is suppressed by increasing fields. Note the strong suppression in  $T_\theta$  in this field range; at some frequencies, the suppression in  $T_\theta$  can be followed over 5 orders of magnitude. Unlike the low-frequency behavior,  $T_\theta$  at high frequency extrapolates toward zero near  $B_{\text{cross}}$ . This latter finding differs from previous microwave cavity measurements on a more disordered  $\text{InO}_x$  film [10]. In that work, the finite-frequency  $T_\theta$  was nonzero well past the phenomenologically defined  $B_{\text{cross}}$  into the strongly insulating phase. This was interpreted as an insulator with localized Cooper pairs, a state that while strongly insulating on long length scales has superconducting correlations on short ones. In contrast, for this low-disorder film,  $T_\theta$  in the high-frequency limit vanishes on approaching  $B_{\text{cross}}$ . This indicates that the superconducting correlations do not survive appreciably across  $B_{\text{cross}}$ , and the superfluid density is indistinguishable from zero into the weakly insulating state as  $T \rightarrow 0$ .

To form a more quantitative understanding of the fluctuations, we fit  $G_1$  and  $G_2$  to a model where the fluctuation contribution is given by a zero-frequency Lorentzian line shape [41]. The fitted width is the characteristic fluctuation rate  $\Omega$  [33]. This is simpler but essentially equivalent to the

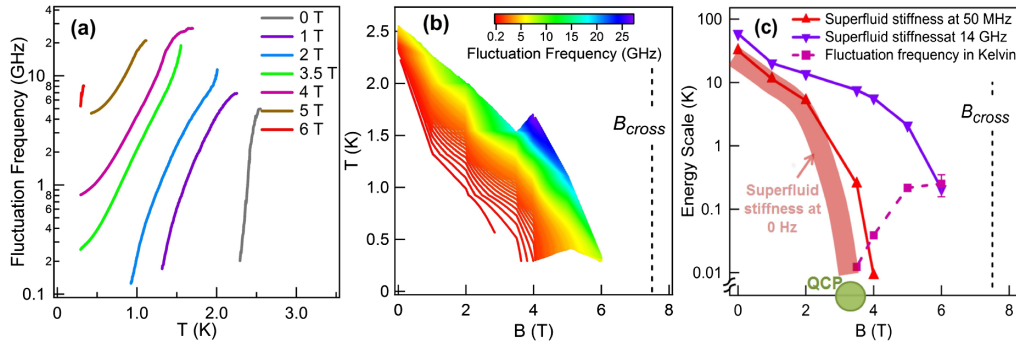


FIG. 4 (color online). (a) Temperature dependence of  $\Omega$  at different fields. (b) Contour plot of  $\Omega$  in temperature and field. Color indicates the magnitude of interpolated values of  $\Omega$  from the fitted data. (c) A phase diagram of all the quantities converted to units of Kelvin. This phase diagram can be extrapolated to  $T = 0$  since most of the quantities in the phase diagram saturate at low temperatures. The dashed vertical black lines in (b) and (c) mark  $B_{\text{cross}}$ .

scaling analysis we performed previously [39]. The use of the Lorentzian line shape is not overly restrictive and only requires the assumption that the charge currents relax exponentially in time. The fits agree well with the data [33], thus justifying this assumption.

In Fig. 4(a), we plot  $\Omega(T)$  for fields up to 6 Tesla. Data above 6 Tesla exhibit fluctuation rates that are far above our accessible frequency range. At zero field,  $\Omega$  goes to zero when  $T$  approaches  $T_c$  from above, showing the critical slowing down that confirms our previous results [39].  $\Omega$  drops in a much slower fashion at finite fields and even begins to saturate to a finite value as  $T \rightarrow 0$  for  $B \gtrsim 3.5$  Tesla. Figure 4(b) is a contour plot of  $\Omega$  in field and temperature. Contours give lines of constant  $\Omega$ . It is safe to conclude that the  $\Omega = 0$  contour falls below the lowermost curve, which is  $\Omega = 0.2$  GHz. In general, small  $\Omega$  contours extrapolate to zero temperature at a field less than 4 Tesla, which is again much smaller than  $B_{\text{cross}}$ .

To form a global view of the zero-temperature behavior, we bring a number of quantities measured at the base temperature together in the phase diagram in Fig. 4(c). For all quantities, energy scales and frequencies have been converted to energy units (in degrees Kelvin). Since these quantities in the phase diagram have little temperature dependence at low temperatures, this phase diagram can be extrapolated to  $T = 0$ . In Fig. 4(c), upward and downward triangles show the low- (50 MHz) and high- (14 GHz) frequency limits of  $T_\theta$  in the accessible frequency range of our setup. The hypothetical behavior of  $T_\theta$  in the zero-frequency limit and the measured  $\Omega(T)$  at base temperatures [the thick line and squares, respectively, in Fig. 4(c)] converge toward zero at  $B \approx 3$  Tesla. This V-shaped phase diagram is exactly what one expects near a QCP where energy scales extrapolate to zero from either side. Again,  $B_{\text{cross}}$ , which is conventionally considered to be a QCP, appears to be completely unrelated to the actual critical behavior. One can see that  $B_{\text{cross}}$  is the field scale where the high-frequency  $T_\theta$  is suppressed. Because of

the lack of evidence for a diverging sheet resistance at  $B_{\text{sm}} < B < B_{\text{cross}}$  in the zero-temperature limit, one reasonable interpretation of the phase diagram is that this low-disorder  $\text{InO}_x$  film has a true QCP [the green dot in Fig. 4(c)] located at  $B_{\text{sm}} \approx 3$  Tesla between a superconducting and an anomalous 2D metallic state. The finite  $T_\theta$  at finite frequencies indicates the existence of superconducting response on the short length scales in this metallic phase. Therefore, the 2D QPT here is characterized by the loss of global coherence in the phase of the superconducting order parameter. Dissipation may occur through quantum delocalized vortices at  $T = 0$  [15–19]. In this picture,  $B_{\text{cross}}$  only marks a crossover in behavior between a metallic state with strong superconducting correlations on short length scales and one with vanishing such correlations.

To conclude, we find evidence for a scenario where a 2D QPT in *weakly* disordered films occurs at a field  $B_{\text{sm}}$  instead of  $B_{\text{cross}}$ . Although this observation runs counter to prevailing dogma in the field, we propose  $B_{\text{sm}}$  as the QCP and a reexamination of the previous scaling analysis of transport properties in such samples. Our results have relevance to many other systems, including high-temperature superconductors and interface superconductivity. The future direction of our project is to perform a careful and complete investigation of more disordered films to compare the effects of different disorder levels.

We thank S. Chakravarty, M. Feigel'man, T. Giamarchi, A. Kapitulnik, S. Kivelson, N. Markovic, K. Michaeli, S. Sachdev, Z. Tesanovic, J.-M. Triscone, and R. Valdes Aguilar for helpful discussions. The research at J.H.U. and U.B. was supported by NSF DMR-0847652 and DMR-0847324, respectively. L.P. was supported by Grant No. GBMF2628 to N.P.A. from the Gordon and Betty Moore Foundation.

*Note added.*—Recently, we became aware of a new Letter using two-coil mutual inductance measurements of field-tuned  $\text{InO}_x$  and  $\text{MoGe}$  films [42]. They also observed that the true critical field is smaller than  $B_{\text{cross}}$ .

- [1] E. Abrahams, P.W. Anderson, D.C. Licciardello, and T.V. Ramakrishnan, *Phys. Rev. Lett.* **42**, 673 (1979).
- [2] A.M. Finkelstein, *Pis'ma Zh. Eksp. Teor. Fiz.* **45**, 3740 (1987) [*JETP Lett.* **45**, 46 (1987)]; *Physica (Amsterdam)* **197B**, 636 (1994).
- [3] M.P.A. Fisher, *Phys. Rev. Lett.* **65**, 923 (1990).
- [4] S. Sondhi, S. Girvin, J. Carini, and D. Shahar, *Rev. Mod. Phys.* **69**, 315 (1997).
- [5] A. Goldman and N. Marković, *Phys. Today* **51**, No. 11, 39 (1998); A. Goldman, *Int. J. Mod. Phys. B* **24**, 4081 (2010).
- [6] V.F. Gantmakher and V.T. Dolgoplov, *Phys. Usp.* **53**, 1 (2010).
- [7] G. Sambandamurthy, L.W. Engel, A. Johansson, and D. Shahar, *Phys. Rev. Lett.* **92**, 107005 (2004).
- [8] A. Pourret, H. Aubin, J. Lesueur, C. Marrache-Kikuchi, L. Berge, L. Dumoulin, and K. Behnia, *Nat. Phys.* **2**, 683 (2006).
- [9] M. Stewart, A. Yin, J. Xu, and J. Valles, *Science* **318**, 1273 (2007).
- [10] R. Crane, N.P. Armitage, A. Johansson, G. Sambandamurthy, D. Shahar, and G. Grüner, *Phys. Rev. B* **75**, 184530 (2007).
- [11] B. Sacépé, C. Chapelier, T.I. Baturina, V.M. Vinokur, M.R. Baklanov, and M. Sanquer, *Phys. Rev. Lett.* **101**, 157006 (2008); B. Sacépé, T. Dubouchet, C. Chapelier, M. Sanquer, M. Ovidia, D. Shahar, M. Feigelman, and L. Ioffe, *Nat. Phys.* **7**, 239 (2011).
- [12] H.M. Jaeger, D.B. Haviland, B.G. Orr, and A.M. Goldman, *Phys. Rev. B* **40**, 182 (1989).
- [13] Y. Liu, D.B. Haviland, L.I. Glazman, and A.M. Goldman, *Phys. Rev. Lett.* **68**, 2224 (1992).
- [14] A. Yazdani and A. Kapitulnik, *Phys. Rev. Lett.* **74**, 3037 (1995).
- [15] D. Ephron, A. Yazdani, A. Kapitulnik, and M.R. Beasley, *Phys. Rev. Lett.* **76**, 1529 (1996).
- [16] J.A. Chervenak and J.M. Valles, *Phys. Rev. B* **61**, R9245 (2000).
- [17] S. Okuma, Y. Imamoto, and M. Morita, *Phys. Rev. Lett.* **86**, 3136 (2001).
- [18] Y. Seo, Y. Qin, C.L. Vicente, K.S. Choi, and J. Yoon, *Phys. Rev. Lett.* **97**, 057005 (2006).
- [19] Y.H. Lin, J.J. Nelson, and A.M. Goldman, *Phys. Rev. Lett.* **109**, 017002 (2012).
- [20] H.S.J. van der Zant, W.J. Elion, L.J. Geerligs, and J.E. Mooij, *Phys. Rev. B* **54**, 10081 (1996); C.D. Chen, P. Delsing, D.B. Haviland, Y. Harada, and T. Claeson, *Phys. Rev. B* **51**, 15 645 (1995).
- [21] S. Eley, S. Gopalakrishnan, P. Goldbart, and N. Mason, *Nat. Phys.* **8**, 59 (2011).
- [22] N. Reyren, S. Thiel, A.D. Caviglia, L. Fitting Kourkoutis, G. Hammerl, C. Richter, C.W. Schneider, T. Kopp, A.-S. Rüetschi, D. Jaccard *et al.*, *Science* **317**, 1196 (2007).
- [23] S. Gariglio and J.-M. Triscone (private communication).
- [24] M. Steiner and A. Kapitulnik, *Physica (Amsterdam)* **422C**, 16 (2005); M.A. Steiner, N.P. Breznay, and A. Kapitulnik, *Phys. Rev. B* **77**, 212501 (2008).
- [25] D. Das and S. Doniach, *Phys. Rev. B* **60**, 1261 (1999).
- [26] N. Mason and A. Kapitulnik, *Phys. Rev. Lett.* **82**, 5341 (1999).
- [27] A. Kapitulnik, N. Mason, S.A. Kivelson, and S. Chakravarty, *Phys. Rev. B* **63**, 125322 (2001).
- [28] P. Phillips and D. Dalidovich, *Phys. Rev. B* **65**, 081101 (2002).
- [29] V.M. Galitski, G. Refael, M.P.A. Fisher, and T. Senthil, *Phys. Rev. Lett.* **95**, 077002 (2005).
- [30] D.B. Haviland, Y. Liu, and A.M. Goldman, *Phys. Rev. Lett.* **62**, 2180 (1989).
- [31] Y. Liu, K.A. McGreer, B. Nease, D.B. Haviland, G. Martinez, J.W. Halley, and A.M. Goldman, *Phys. Rev. Lett.* **67**, 2068 (1991).
- [32] Wei Liu, Ph.D. thesis, Johns Hopkins University, 2013; Wei Liu, LiDong Pan, and N.P. Armitage (to be published).
- [33] See Supplemental Material at <http://link.aps.org/supplemental/10.1103/PhysRevLett.111.067003> for details.
- [34] V. Gantmakher and M. Golubkov, *JETP Lett.* **73**, 131 (2001).
- [35] J.C. Booth, D.H. Wu, S.B. Qadri, E.F. Skelton, M.S. Osofsky, A. Piqué, and S.M. Anlage, *Phys. Rev. Lett.* **77**, 4438 (1996).
- [36] M. Lee and M.L. Stutzmann, *Phys. Rev. Lett.* **87**, 056402 (2001).
- [37] M. Scheffler and M. Dressel, *Rev. Sci. Instrum.* **76**, 074702 (2005).
- [38] T. Ohashi, H. Kitano, I. Tsukada, and A. Maeda, *Phys. Rev. B* **79**, 184507 (2009).
- [39] W. Liu, M. Kim, G. Sambandamurthy, and N.P. Armitage, *Phys. Rev. B* **84**, 024511 (2011).
- [40] G. Sambandamurthy, A. Johansson, E. Peled, D. Shahar, P. Björnsson, and K. Moler, *Europhys. Lett.* **75**, 611 (2006).
- [41] A. Kuzmenko, *Rev. Sci. Instrum.* **76**, 083108 (2005).
- [42] S. Misra, L. Urban, M. Kim, G. Sambandamurthy, and A. Yazdani, *Phys. Rev. Lett.* **110**, 037002 (2013).